Original Article

Treatment of chronic obstructive pulmonary disease by traditional Chinese medicine Morin monomer regulated by autophagy

Zhen Liu^, Yang Zeng, Rui Li, Ying Yan, Sicheng Yi, Kui Zhang^

Department of Traditional Chinese Medicine, Guizhou Provincial People's Hospital, Guiyang, China

Contributions: (I) Conception and design: Z Liu, K Zhang; (II) Administrative support: K Zhang; (III) Provision of study materials or patients: Z Liu, Y Zeng, R Li; (IV) Collection and assembly of data: Z Liu, Y Zeng, R Li, Y Yan, S Yi; (V) Data analysis and interpretation: Z Liu, Y Zeng, R Li, Y Yan, S Yi; (VI) Manuscript writing: All authors; (VII) Final approval of manuscript: All authors.

Correspondence to: Kui Zhang, MD. Department of Traditional Chinese Medicine, Guizhou Provincial People's Hospital, No. 83 Zhongshan East Road, Guiyang 550002, China. Email: zky0696@163.com.

Background: Chronic obstructive pulmonary disease (COPD) is a frequently occurring disorder. The aim of this study is to explore the mechanism of traditional Chinese medicine Morin monomer in the treatment of COPD via regulating autophagy based on the long non-coding RNA (lncRNA) H19/microRNA (miR)-194-5p/Sirtuin (SIRT)1 signal axis.

Methods: The COPD rat model was constructed, and the lung tissues were collected. The pathological analysis was performed using hematoxylin-eosin (HE), Masson, and periodic acid-Schiff (PAS) staining. Autophagosomes were observed using transmission electron microscope. *LncRNA H19*, *miR-194-5p*, *SIRT1* genes in the rat lung tissues were detected using reverse transcription-quantitative real-time polymerase chain reaction (RT-qPCR). The autophagy-related proteins including SIRT1, mammalian/mechanistic target of rapamycin (mTOR), phosphorylated (p)-mTOR, microtubule-associated protein light chain 3 (LC3), Beclin-1, autophagy-related (ATG)7, and p62 in each group were detected using Western blot.

Results: The rats in the control group had normal lung structure. Alveolar enlargement and destruction could be found in the rat lung tissues in the model group, accompanied with obvious infiltration of inflammatory cells, thickened bronchial walls, enlarged alveolar septum, collagen fibers deposition, and goblet cells proliferation. In comparison with the model group, Morin treatment relieved the lung injuries, which was optimized in the moderate- and high-dose groups. The number of autophagosomes in the lung tissues of the model rats was dramatically increased compared with the normal rats. However, the number of autophagosomes in each Morin treatment group was obviously less than that in the model group. *LncRNA H19* and *SIRT1* expression was significantly increased in the model group, and *miR-194-5p* was significantly decreased ($P<0.05$). Morin and 3-methyladenine (3-MA) could obviously reduce the *lncRNA H19* and *SIRT1* expression, and increase the *miR-194-5p* expression ($P<0.05$). Relative to control rats, ATG7, Beclin-1, LC3II/I and SIRT1 levels in the model group increased obviously, while the expression of p62, and p-mTOR/mTOR decreased ($P<0.05$). Morin treatment reduced the expression of ATG7, Beclin-1, SIRT1, LC3II/I significantly, and increased the p-mTOR/mTOR and p62 expression ($P<0.05$).

Conclusions: Morin decreased *lncRNA H19* expression, resulting in upregulation of *miR-194-5p* expression, downregulation of *SIRT1* expression, and increased of p-mTOR/mTOR expression. Furthermore, cell autophagy was inhibited, contributing to the COPD treatment.

Keywords: Chronic obstructive pulmonary disease (COPD); autophagy; long non-coding RNA H19 (lncRNA H19); microRNA-194-5p/Sirtuin 1 (miR-194-5p/SIRT1)

^ ORCID: Zhen Liu, 0009-0000-8169-5358; Kui Zhang, 0009-0003-2564-8380.

Submitted Dec 03, 2023. Accepted for publication Aug 06, 2024. Published online Sep 26, 2024.
doi: 10.21037/jtd-23-1836
View this article at: https://dx.doi.org/10.21037/jtd-23-1836

Introduction

Chronic obstructive pulmonary disease (COPD) is a kind of frequently occurring disorder, seriously endangering human health. COPD is featured by the airway obstruction that is incomplete or irreversible, generally accompanied by alveolar destruction and mucous metaplasia. As a complex disease, COPD is affected by multiple factors, including genetic-environmental factor interactions, however, its underlying pathogenic mechanism remains unknown (1). Influenced by air pollution, dust, smoking and aging, the incidence of COPD is progressively rising.

Autophagy, a lysosome-dependent degradation process in eukaryotic cells, has a key function in maintaining cell homeostasis. Under normal physiological conditions, almost all cells have a basic level of autophagy, which could eliminate unfolded or misfolded proteins, and degrade proteins to generate amino acids for cell recirculation (2). Cell damage and programmed death caused by excessive autophagy or autophagy dysfunction exert a significant influence on disease onset and progression.

Mulberry (*Morus* L.) has been a traditional Chinese medicine since ancient China. Recently, numerous researches have demonstrated that mulberry branches contain a variety of bioactive components, such as alkaloids, phenols, polysaccharides, and flavonoids. Modern pharmacological studies also proved the anti-inflammatory, hypoglycemic, hypotensive, anticarcinogenic and anti-microbial activities of multiple extracts from Cortex Mori (3-5).

The abnormal expression of long non-coding RNA (lncRNA) has been confirmed to play an important role in the occurrence and development of various diseases, including COPD (6). Many lncRNAs that play a role in COPD have been discovered, for example, knocking out lncRNA taurine upregulated gene 1 (*TUG1*) can alleviate lung inflammatory damage in COPD (7,8). MicroRNAs (miRNAs) are also a subclass of non-coding RNAs, and the current research focus on miRNAs is their sponge adsorption by upstream lncRNAs, which leads to inhibition of biological functions (9). A study reported that *lncRNA H19* leads to smoking related COPD by targeting the *miR-181*/programmed cell death protein (PDCD)4 axis (10). In addition, in non-small cell lung cancer patients with COPD, *lncRNA H19* and *miR-675* levels are significantly upregulated (11).

In this study, we investigated the mechanism of Morin on cell autophagy in COPD rats. We aimed to study the mechanism of Morin in the treatment of COPD by regulating autophagy through *lncRNA H19*/*miR-194-5p*/Sirtuin 1 (*SIRT1*) expression. A COPD rat model was established. The ultrastructure of the epithelial cells and autophagosomes was observed under a transmission electron microscope (TEM). The *lncRNA H19*, *miR-194-5p*, and *SIRT1* levels in each group were measured, and the downstream signaling pathways were detected with Western blot (WB). The findings of this study may provide a reference for the detection of new molecular targets for the prevention and treatment of COPD. We present this article in accordance with the ARRIVE reporting checklist (available at https://jtd.amegroups.com/article/view/10.21037/jtd-23-1836/rc).

Highlight box

Key findings

- Morin inhibited cell autophagy of chronic obstructive pulmonary disease (COPD) rat model through regulating the *lncRNA H19*/*miR-194-5p*/*SIRT1* expression.

What is known and what is new?

- Cigarette smoke extract could lead to autophagy and COPD. Morin, a traditional Chinese medicine has a good therapeutic effect on COPD.
- Morin could obviously reverse the effect of COPD rat model.

What is the implication, and what should change now?

- Morin is a potential treatment for COPD.
- Further studies may investigate the mechanisms more in depth.

Methods

Animals and reagents

Thirty-six specific-pathogen-free (SPF) Sprague-Dawley (SD) rats (male, 230–270 g) were purchased from Hunan SJA Laboratory Animal Co., Ltd [Certificate No. SCXK (Xiang) 2019-0004]. The rats were raised in cages under 20–26 ℃, humidity 40–70%, and *ad libitum* to SPF

grade animal feed and sterilized drinking. Cigarette was purchased from China Tobacco Jiangxi Industrial LLC. Morin (Cat#654055-01-3) and 3-methyladenine (3-MA) (Cat#5142-23-4) was provided by Shanghai Yuanye Bio-Technology Co., Ltd. (Shanghai, China). Hematoxylin (Cat#ZLI-9610) was from ZSGB-Bio Inc., Beijing, China. Eosin (Cat#G1100), Modified Masson's Trichrome Stain Kit (Cat#G1345), and periodic acid-Schiff (PAS) Stain Kit (Cat#G1281) were from Solarbio, Beijing, China. Trizon Reagent (Cat#CW0580S), Ultrapure RNA Kit (Cat#CW0581M), miRNA complementary DNA (cDNA) Synthesis Kit (Cat#CW2141S), miRNA quantitative polymerase chain reaction (qPCR) Assay Kit (Cat#CW2142S) and miRNA Purification Kit (Cat#CW0627S) were from CoWin Biosciences (CWBIO). Hiscript II Q RT SuperMix for qPCR (Cat#R223-01) was provided by Vazyme, Nanjing, China. 2× SYBR Green PCR Master Mix (Cat#A4004M) was provided by Xiamen LifeInt Technology Co., Ltd. (Xiamen, China).

Experimental grouping

A protocol was prepared before the study without registration. The protocol of this study was approved by the Ethics Committee of Guizhou Provincial People's Hospital (approval No. 202021-010), and conducted in compliance with the institutional guidelines for the care and use of animals. The rats were randomly allocated into control, model group, low-dose Morin (25 mg/kg/d), medium-dose Morin (50 mg/kg/d), high-dose Morin (100 mg/kg/d), and 3-MA (15 mg/kg/d) groups (n=6/group). Randomization sequence was generated using random-number table. The dose for Morin was obtained based on previous studies (12,13). All experiments were conducted in the laboratory. The investigators performing the subsequent experiments and data analysis were blinded to the grouping allocation.

COPD modeling

The rats were anesthetized with an intraperitoneal injection of 1% of pentobarbital sodium (3 mL/kg) and received 0.2 mL intratracheal instillation of lipopolysaccharides (LPS) on the 1st and the 14th day. After injection, the rats were rotated upright for 1 min to distribute the LPS evenly in the lungs. Cigarette smoke exposure was given in a passive smoking chamber with 1 cigarette for 30 min once a day for each rat from the 2nd to 13th day and 15th to 28th day, respectively.

The rats in the low-dose Morin group received Morin suspension (5 mg/mL) by oral gavage (0.5 mL/100 g) on the 15th day for six consecutive weeks (25 mg/kg/d). The rats in the medium-dose Morin group received Morin suspension (5 mg/mL) by oral gavage (1 mL/100 g) on the 15th day for six consecutive weeks (50 mg/kg/d). The rats in the high-dose Morin group received Morin suspension (10 mg/mL) by oral gavage (1 mL/100 g) on the 15th day for six consecutive weeks (100 mg/kg/d).

The rats in the 3-MA group received intraperitoneal injection of 3-MA solution (5 mg/mL) on the 15th day for six consecutive weeks (15 mg/kg/d).

After completed treatment, the rats were anesthetized. Blood samples were obtained from the abdominal aorta. The lung tissues were taken.

Tissue preparation and hematoxylin-eosin (HE) staining

The lung tissues were gathered and fixed with 10% paraformaldehyde. The tissue sections were gradient dehydrated using ethyl alcohol, cleared with xylene, and immersed in paraffin. A 4 μm paraffin section was then prepared, followed by 3 min of hematoxylin staining, rinsed with deionized water, followed by 15 s of differentiation with differentiation fluid. Then, the section was subjected to 3 min of eosin staining and 3 min of soaking with tap water. Subsequently, gradient alcohol was used to dehydrate the section for 2 min, followed by clearing with xylene for 20 min and sealing with neutral gum. Light microscope (CX41; Olympus, Japan) was used to capture images.

Masson staining

Masson staining was performed in accordance with the manufacturer's protocol. Sections were incubated with Bouin solution for 2 h under 37 ℃, followed by 3 min of celestite blue staining. After 10 s of rinsing with deionized water, the sections were subjected to 10 min of Ponceau solution staining, 6 min of phosphomolybdic acid solution staining, and 20 min of aniline blue staining, followed by 2 min of gradient ethanol dehydration (95%, 100%). Xylene was used to clear the sections for 2 min thrice. Then, the tissue slices were sealed with neutral resin. Finally, the images were acquired using a light microscope (CX41; Olympus).

Glycogen PAS staining

The lung tissue sections were dehydrated and washed with

Table 1 Primer information

Gene	Primer sequence (5' to 3')	Primer length (nt)	Production length (bp)	Temp (℃)
miR-194-5p R	GTCGTATCCAGTGCAGGGTCCGAGGTATTCGCACTGGATAC GACTCCACA	50	–	–
miR-194-5p F	CGCGTGTAACAGCAACTCCA	20	66	59.5
miR-194-5p R	AGTGCAGGGTCCGAGGTATT	20		
lncRNA H19 F	GCGGGTCTGTTTCTTTACTTC	21	258	53.2
lncRNA H19 R	TTCCGATGGTGTCTTTGATG	20		
SIRT1 F	TAGGCGGCTTGATGGTAATC	20	142	57.7
SIRT1 R	CTGGCATGTCCCACTATCAC	20		
β-actin F	TGGCACCCAGCACAATGAA	20	186	60.8
β-actin R	CTAAGTCATAGTCCGCCTAGAAGCA	20		
U6 F	CTCGCTTCGGCAGCACA	17	90	57.3
U6 R	AACGCTTCACGAATTTGCGT	20		

tap water for 3 min. The sections were stained with periodic acid for 7 min at room temperature, subjected to Schiff reagent for 15 min in the dark, and followed by hematoxylin staining for 3 min at room temperature. After differentiation with acidic differentiation fluid for 2–5 s, a 10 min washing was performed with tap water, and the images were obtained using a light microscope (CX41; Olympus).

Transmission electron microscopy (TEM) detection

The collected lung tissues were subjected to 2 h of fixation with 2.5% glutaraldehyde plus 2% paraformaldehyde, followed by another 2 h of post-fixation with 1% OsO_4 under 4 ℃. Thereafter, each sample was treated with gradient ethanol dehydration and epoxy resin embedding. Subsequently, the 1-μm sections were prepared, followed by 1% toluidine blue staining. A representative block was selected for ultrathin sectioning. Subsequently, 70-nm sections were prepared, followed by double-staining using 7.3% uranyl acetate and lead citrate, and observed under a TEM [JEM-1230 (80 KV), JEOL].

Reverse transcription-quantitative real-time PCR (RT-qPCR)

Extraction of miRNA and total RNA from rat lung tissues in each group was performed using TRIzol reagent in line with the manufacturer instructions. The concentration of RNA was detected and cDNAs were prepared. All primers involved in the present study are presented in *Table 1*. CFX Connect™ Real-Time PCR detection system (Bio-Rad Laboratories, Inc., USA) was adopted for PCR under the following conditions, 10 min of predenaturation under 95 ℃, 10 s of denaturation under 95 ℃, 30 s of annealing under 58 ℃, and 30 s of extension under 72 ℃, for 40 cycles. The gene expression was quantified by $2^{-\Delta\Delta Ct}$ method. The results were shown as the fold changes of specific genes compared with the control group.

WB detection

The lung tissues of rats in each group were collected and lysed on ice. Tissue lysis was maintained for 20 min on ice, followed by 10 min of centrifugation at 12,000 rpm. Besides, the concentrations of extracted protein of each group were estimated with a bicinchoninic acid (BCA) protein assay kit. After 15 min of protein denaturation under 85 ℃, they were separated by sodium dodecyl sulphate-polyacrylamide gel electrophoresis (SDS-PAGE) for 2 h and transferred onto the 0.45-mm polyvinylidene fluoride (PVDF) membranes.

Then, 5% nonfat milk contained within Tris-buffered saline (TBS) was used to block non-specific binding under 4 ℃ overnight. Then, the primary antibodies were used to incubate the PVDF membranes under 37 ℃ for 1 h. Subsequently, horseradish peroxidase (HRP)-labeled secondary antibodies were used to further incubate the PVDF membranes at room temperature for 1 h. The enhanced chemiluminescence reagent kit was used to detect

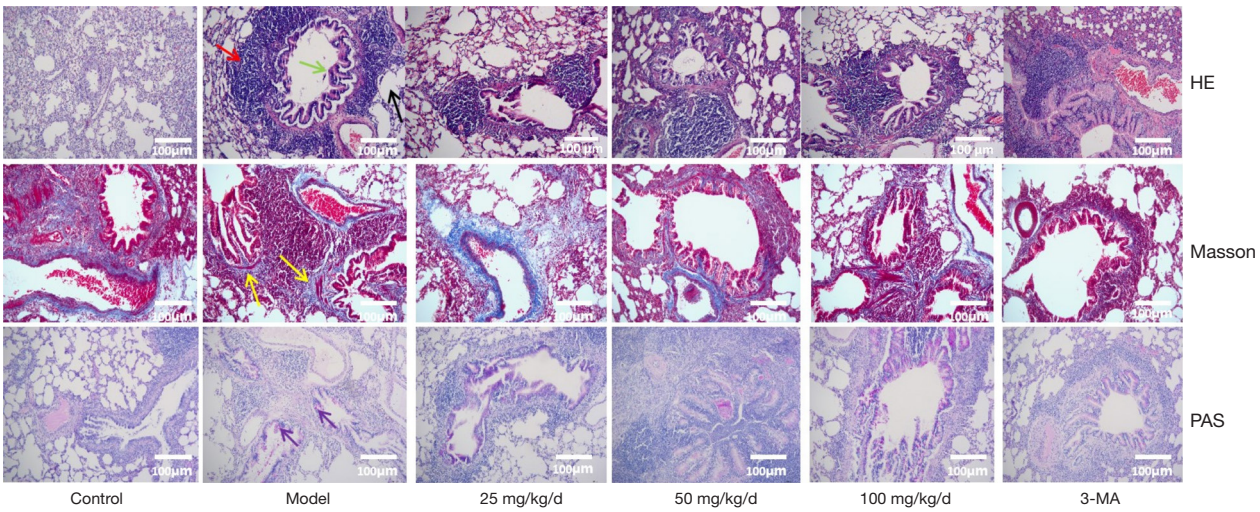

Figure 1 Histological examination results detected using HE, Masson and PAS staining on the lung tissues of rats in each group (×200) (n=6/group). The lung structure of the rats in the control group is normal. In the model group, the pulmonary alveoli of rats were not completely expanded (black arrow), the inflammatory cells were significantly infiltrated (red arrow), the bronchial tube wall was significantly thickened (green arrow), the alveolar septum was thickened and a large number of collagen fibers were deposited (yellow arrows), and the goblet cells were significantly proliferated (purple arrows). Compared with the model group, different degrees of relief were observed under light microscopy in each treatment group, with the medium- and high-dose Morin groups being the most significant. HE, hematoxylin-eosin; PAS, periodic acid-Schiff.

specific bands according to the manufacturer's protocol. The bands were analyzed using ImageJ.

Statistical analysis

The data were presented as mean ± standard deviation (SD) and explored with Graphpad Prism 7. One-way analysis of variance (ANOVA) were used to investigate the significant differences between samples. For all tests, $P<0.05$ was set as the level of significance.

Outcome measures

- The effect of Morin on lung tissues of COPD rats in lung histological examination was observed by HE, Masson and PAS staining.
- The effect of Morin on autophagy in lung tissues of COPD rats was observed using TEM.
- The effect of Morin on the expression of *lncRNA H19*, *miR-194-5p*, and *SIRT1* genes in lung tissues of COPD rats was detected with RT-qPCR.
- The effect of Morin on the expression of SIRT1, mammalian/mechanistic target of rapamycin (mTOR), phosphorylated (p)-mTOR, microtubule-associated protein light chain 3 (LC3), Beclin-1, autophagy-related (ATG)7 and p62 proteins in lung tissues of COPD rats was determined using WB.

Results

The effect of Morin on lung tissues of COPD rats in lung histological examination

To evaluate the therapeutic effects of Morin and autophagy inhibitor 3-MA on COPD rat model, the rat lung tissues in each group were gathered and stained with HE, Masson, and PAS to observe the pathological changes. As shown in *Figure 1*, the rats in the control group had normal lung structure. The rat lung tissues of the model group showed incomplete alveolar enlargement (black arrow), obvious infiltration of inflammatory cells (red arrow), significant thickening of the bronchial wall (green arrow), thickening of the alveolar septa and deposition of a large amount of collagen fibers (yellow arrows), and significant proliferation of goblet cells (purple arrows). Compared with the model group, different degrees of alleviation were observed under the light microscope in each treatment group; for the Morin treatment group, the medium and high doses Morin are the most obvious.

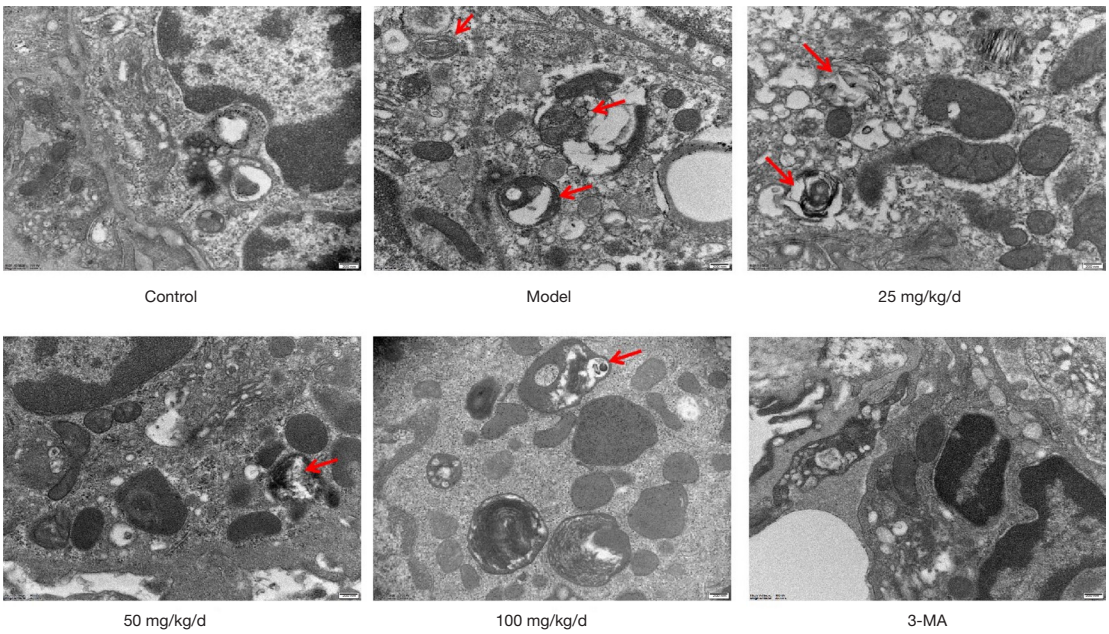

Figure 2 Autophagy in the lung tissues of rats in each group observed using TEM (n=6/group). The autophagosome is indicated by the arrows. Scale bar =200 nm. 3-MA, 3-methyladenine; TEM, transmission electron microscope.

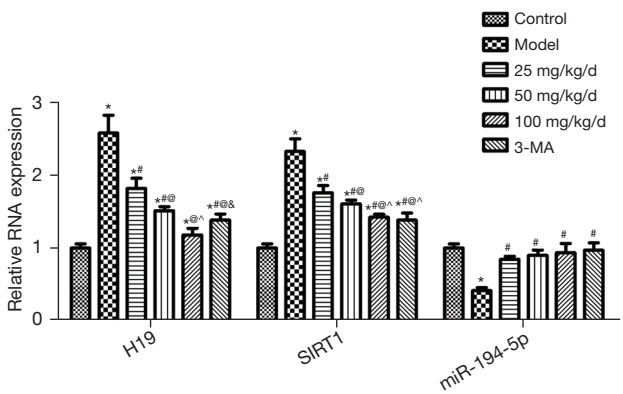

Figure 3 The *lncRNA H19*, *SIRT1* and *miR-194-5p* levels within the lung tissues of rats in each group detected using RT-qPCR (n=6/group). The error bars indicate the mean ± SD. *, P<0.05 and #, P<0.05 relative to blank control and model groups, respectively; @, P<0.05, ^, P<0.05, and &, P<0.05 relative to low-, medium-, and high-dose Morin groups, respectively. LncRNA, long non-coding RNA; miR, microRNA; SIRT, Sirtuin; SD, standard deviation; RT-qPCR, reverse transcription-quantitative real-time polymerase chain reaction; 3-MA, 3-methyladenine.

The effect of Morin on autophagy in lung tissues of COPD rats observed using TEM

The autophagosomes of the lung tissues were observed using TEM and the number of autophagosomes was recorded in every 10 fields at the magnification of 30,000 times. As presented in *Figure 2*, the number of autophagosomes in the lung tissues of the model group rats was obviously more than that in the normal (control) group. However, the number of autophagosomes in each treatment group was obviously less than that in the model group.

The effect of Morin on the expression of lncRNA H19, miR-194-5p, and SIRT1 genes in the lung tissues of COPD rats

RT-qPCR was conducted to measure the *lncRNA H19*, *SIRT1* and *miR-194-5p* expression in the rat lung tissues. As shown in *Figure 3*, the *lncRNA H19* and *SIRT1* expression was significantly increased in the model group, and the *miR-194-5p* expression was significantly decreased (P<0.05).

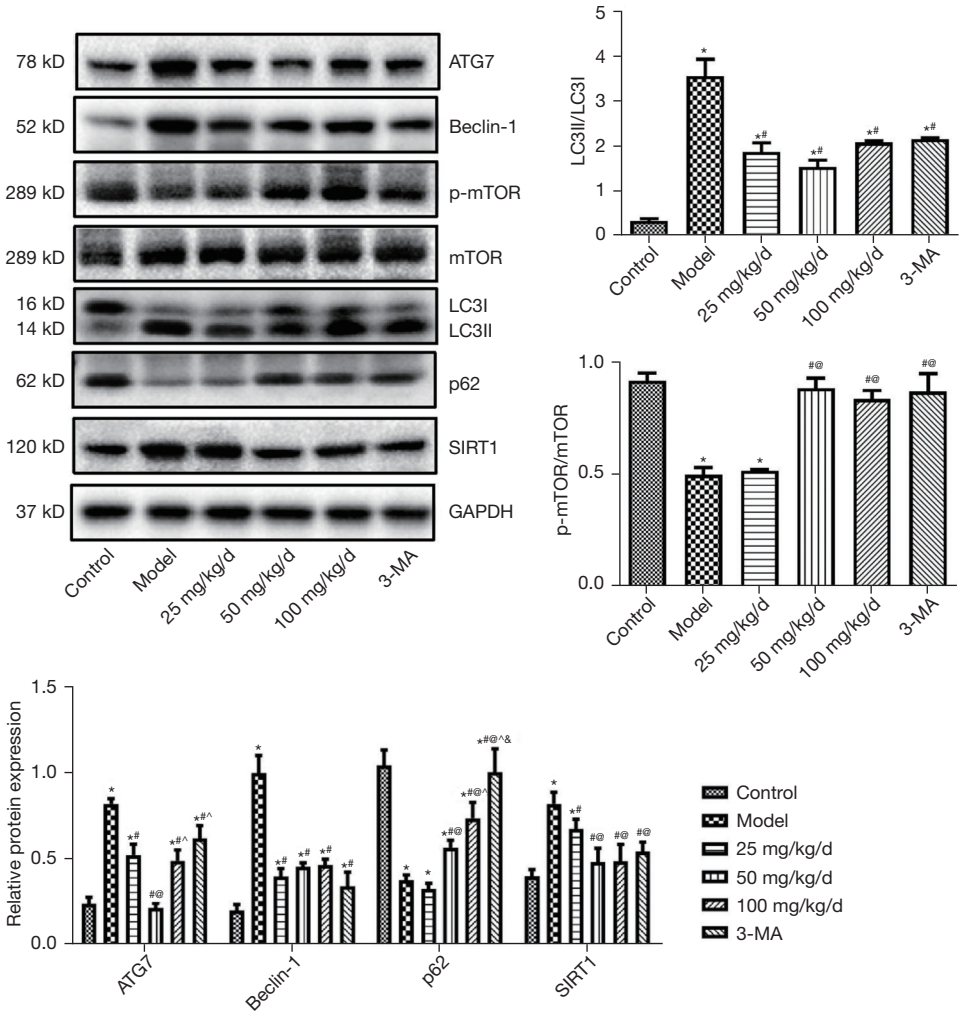

Figure 4 The expression of SIRT1, mTOR, p-mTOR, LC3, Beclin-1, ATG7 and p62 proteins in the lung tissues of rats in each group detected using WB (n=6/group). *, P<0.05 and #, P<0.05 relative to blank control and model groups, respectively; @, P<0.05, ^, P<0.05, and &, P<0.05 relative to low-, medium-, and high-dose Morin groups, respectively. mTOR, mammalian/mechanistic target of rapamycin; p, phosphorylated; LC3, microtubule-associated protein light chain 3; ATG, autophagy-related; WB, Western blot; SIRT, Sirtuin; 3-MA, 3-methyladenine.

Morin and 3-MA could significantly decrease the expression of *lncRNA H19* and *SIRT1*, and significantly increase the *miR-194-5p* expression (P<0.05).

The effect of Morin on the expression of SIRT1, mTOR, p-mTOR, LC3, Beclin-1, ATG7 and p62 proteins in the lung tissues of COPD rats

The expression of the autophagy-related proteins SIRT1, mTOR, p-mTOR, LC3, Beclin-1, ATG7 and p62 in the lung tissues of rats with COPD was detected using WB. According to *Figure 4*, in comparison with the control group, the expression of ATG7, Beclin-1, SIRT1 and LC3II/I in the model group increased significantly, while the expression of p-mTOR/mTOR and p62 decreased significantly (P<0.05). Morin treatment reduced the expression of ATG7, Beclin-1, SIRT1 and LC3II/I, and increased the expression of p-mTOR/mTOR and p62 (P<0.05). Moreover, similar results could be observed in the autophagy inhibitor group.

Discussion

It has been fully demonstrated that smoke leads to inflammation, oxidative stress, and apoptosis. Besides, cell senescence could promote epithelial cell injuries, which result in emphysema, COPD, or serious decline in lung function. However, the key mechanism remains unclear. Therefore, it is urgent to understand the pathogenesis and discover new treatment methods. Cigarette smoking is one of the main reasons for COPD. According to previous studies, cigarette smoke extract (CSE) could lead to autophagy of human airway epithelial cells *in vitro* (14-16). The epithelial cells in the trachea and alveoli are the main targets of inhaled cigarette smoke. The key role of the airway epithelium includes maintenance of a semi-permeable barrier, proper immune monitoring and response to environmental stimuli, as well as the normal survival and turnover with potential progenitor cells. These features are interfered during COPD and in a variety of cigarette smoke exposure models (17). The activation of autophagy and selective autophagy are detrimental mechanisms of epithelial cell responses to smoke (18). Cigarette smoke increases autophagosomes turnover and promotes epithelial cell death, which in turn triggers and exaggerates airway inflammation and mucus hypersecretion (19). Cigarette smoke has been reported to accelerate autophagy, which leads to epithelial cell death (20). Number of studies have reported that smoking can impair epithelial cells and undergo autophagy, leading to the accumulation of defective autophagy complexes and cell senescence (21,22). In this study, the COPD rat model was established by cigarette smoking, and histological test results demonstrated alveolar enlargement and destruction in the rat lung tissues of the model group, accompanied with obvious inflammatory cell infiltration, thickened bronchial walls, enlarged alveolar septum, collagen fibers deposition, and goblet cells proliferation. TEM observation showed that the number of autophagosomes in the lung tissues of the model group was obviously higher than the normal group.

Shenqi Bufei decoction can significantly improve the symptoms of patients with Lung-Qi deficiency syndrome in stable stage of COPD, stabilize lung function and prevent the decline of lung function (23). Previous *in vitro* and *in vivo* experiments confirmed that Shenqi Bufei Decoction can inhibit the proliferation of airway smooth muscle cells in COPD model rats with Lung-Qi deficiency syndrome, and significantly inhibit the thickening of small airway walls (24-26). Shenqi Bufei Decoction is composed of Radix Astragali, Mori Cortex, *Psoralea corylifolia* Linn, *Salvia miltiorrhiza* Bunge, etc. The drug compatibility exerts the effects of replenishing Qi and nourishing lungs, resolving phlegm, and promoting blood circulation, and thus Qi deficiency can be replenished, phlegm and blood stasis can be relieved, the Qi dynamic can be smoothed, and cough and asthma can be relieved. From the three main active components of Cortex Mori, resveratrol, morinone, and morin, through screening of the COPD cell model, it is found that Morin has the best therapeutic effect on COPD (24). Study have also found that Morin can improve COPD by inhibiting matrix metalloproteinase (MMP)9 expression (27). In the present study, Morin at different doses was applied on the COPD rats. Histological and TEM examination found that Morin can improve the pathology of COPD model and reduce the autophagosomes formation, suggesting that the treatment effect of Morin on COPD was achieved via regulating autophagy. Among them, the effect of medium dose and high dose Morin was better.

LncRNA H19 inhibited autophagy in the *in vitro* cell model of oxygen and glucose deprivation/reperfusion (OGD/R) model through dual-specificity phosphatase (DUSP)5-extracellular signal regulated kinase (ERK)1/2 axis (28). *LncRNA H19* is highly expressed in lung cancer tissues and cells, and its overexpression promotes cell migration, invasion, and epithelial-mesenchymal transition via negative regulation of miRNA (29). Bioinformatics analysis shows that *miR-194-5p* can directly bind to *H19*, which has been confirmed in colon cancer (30). Previous studies have demonstrated that many miRNAs are involved in the regulation of autophagy (31-33). *SIRT1* is a direct target of *miR-194-5p*, and is highly expressed in the colorectal cancer, thus promoting autophagy of tumor cells (30). The present study found that *lncRNA H19* and *SIRT1* expression was significantly increased in the COPD rats, whereas the *miR-194-5p* expression was significantly decreased, which could be reversed by Morin treatment. The treatment effect of Morin on COPD could be achieved through regulation of autophagy and the *lncRNA H19/miR-194-5p/SIRT1* signal axis. We would further verify this with dual-luciferase reporter assays in subsequent studies.

ATG regulates autophagosome formation by forming ATG12-ATG5 and LC3II (ATG8-II) complexes. Under the action of ATG7 and ATG10 (corresponding to ubiquitin-activating enzyme E1 and ubiquitin-conjugating enzyme E2, respectively), ATG12 and ATG5 are combined through an ubiquitin-like reaction to form ATG12-ATG5 conjugate,

which then combines with ATG16 through non covalent bond to form ATG12-ATG5-ATG16 complex, which participates in the expansion of autophagosomes (34). Under the action of ATG4, ATG7 and ATG3, LC3 is converted into LC3II-phosphatidylethanolamine (PE) and tightly bound to the surface of the autophagosome membrane, participating in the extension of the pre-autophagosome (35,36). Beclin-1 is an essential molecule for the formation of autophagosomes, and it can mediate the localization of autophagy-related proteins to phagosomes (37,38). By reacting with various proteins, Beclin-1 transmits autophagy signals and regulates the formation and maturation of autophagosomes (39). p62 is a ubiquitin binding protein, which is closely related to protein ubiquitination. It is involved in a variety of cell signal transduction regulation and autophagy processes (40). In the process of autophagy, p62 binds to ubiquitinated proteins, and then forms a complex with LC3II protein localized on the inner membrane of the autophagosomes, which is degraded in autophagolysosomes. Therefore, when autophagy occurs, p62 protein is continuously degraded in the cytoplasm; when autophagy activity is weakened and autophagy function is defective, p62 protein will continue to accumulate in the cytoplasm. p62 is one of the marker proteins reflecting autophagy activity, and its content indirectly indicates the level of autophagosome clearance (41). In the present study, COPD rat model was established to detect the lung tissues, and it was found that compared with the control group, the LC3II/I and Beclin-1 expressions in the COPD group were significantly increased and p62 expression was significantly decreased, indicating that the level of autophagy in the COPD model was increased, which was in consistence with the above studies. The expression of autophagy-related proteins LC3II/I and Beclin-1 was significantly decreased, and the expression of p62 was increased after treatment with Morin. These results also indicated that Morin could regulate autophagy. There is also study showing that insufficient autophagy may lead to accelerated cell senescence in COPD, suggesting that autophagy may also have a protective effect in tobacco smoke induced senescence-associated lung disease, COPD (42). We would investigate this more in depth in future studies to achieve an optimal dose of Morin for COPD treatment.

The mTOR kinase plays an important regulatory role in autophagy response (43). The autophagy response is inhibited when mTOR [AKT and mitogen-activated protein kinase (MAPK) signaling] is activated by mTOR kinases. In contrary, when mTOR [5' adenosine monophosphate-activated protein kinase (AMPK) and p53 signaling] is not inhibited, the autophagy response mechanism is initiated (44). A recent study revealed that SIRT1 can activate the AMPK pathway, which is closely related with the activation of mTOR (45). Typically, the AMPK-mTOR pathway has a critical function in regulating autophagy (46). Activation of AMPK could inhibit the phosphorylation of mTOR, and further promote cell autophagy (47). In this study, the results showed that the expression of p-mTOR/mTOR in the COPD rat model was significantly decreased, indicating that COPD inhibited the phosphorylation of mTOR. Morin treatment could increase the expression of p-mTOR/mTOR, suggesting that Morin could promote phosphorylation of mTOR, thereby inhibited autophagy.

This study mainly investigated the mechanism of Morin on cell autophagy in COPD rats. Future studies will evaluate the relationship between *lncRNA H19*, *SIRT1*, ATG7, Beclin-1, LC3II/I, *miR-194-5p*, p62, and p-mTOR/mTOR, and the mechanisms will be investigated more in depth. Quantitative pathology of the histopathological test will also be performed.

Conclusions

Morin treatment plays a therapeutic role in COPD through the signaling pathway regulated by H19. Morin decreased *lncRNA H19* expression, upregulated *miR-194-5p* and downregulated target gene *SIRT1* expression, increased p-mTOR/mTOR expression and inhibited cell autophagy of COPD rat model.

Acknowledgments

Funding: This work was supported by the National Natural Science Foundation of China (grant No. 81960892).

Footnote

Reporting Checklist: The authors have completed the ARRIVE reporting checklist. Available at https://jtd.amegroups.com/article/view/10.21037/jtd-23-1836/rc

Data Sharing Statement: Available at https://jtd.amegroups.com/article/view/10.21037/jtd-23-1836/dss

Peer Review File: Available at https://jtd.amegroups.com/article/view/10.21037/jtd-23-1836/prf

Conflicts of Interest: All authors have completed the ICMJE uniform disclosure form (available at https://jtd.amegroups.com/article/view/10.21037/jtd-23-1836/coif). The authors have no conflicts of interest to declare.

Ethical Statement: The authors are accountable for all aspects of the work in ensuring that questions related to the accuracy or integrity of any part of the work are appropriately investigated and resolved. The protocol of this study was approved by the Ethics Committee of Guizhou Provincial People's Hospital (approval No. 202021-010), and conducted in compliance with the institutional guidelines for the care and use of animals.

References

1. Salvi S. Tobacco smoking and environmental risk factors for chronic obstructive pulmonary disease. Clin Chest Med 2014;35:17-27.
2. Takabatake Y, Kimura T, Takahashi A, et al. Autophagy and the kidney: health and disease. Nephrol Dial Transplant 2014;29:1639-47.
3. Weng YJ, Zhang M, Wang J, et al. Significantly hypoglycemic effect of a novel functional bread rich in mulberry bark and improving the related functions of liver, pancreas, and kidney, on T2D mice. Food Sci Nutr 2021;9:2468-82.
4. He Y, Cun S, Fan J, et al. Screening for promising multi-target bioactive components from Cortex Mori Radicis for the treatment of chronic cor pulmonale based on immobilized beta(1)-adrenergic receptor and beta(2)-adrenergic receptor chromatography. J Chromatogr B Analyt Technol Biomed Life Sci 2024;1242:124175.
5. Hu X, Zhang K, Pan G, et al. Cortex Mori extracts induce apoptosis and inhibit tumor invasion via blockage of the PI3K/AKT signaling in melanoma cells. Front Pharmacol 2022;13:1007279.
6. Wang Y, Chen J, Chen W, et al. LINC00987 Ameliorates COPD by Regulating LPS-Induced Cell Apoptosis, Oxidative Stress, Inflammation and Autophagy Through Let-7b-5p/SIRT1 Axis. Int J Chron Obstruct Pulmon Dis 2020;15:3213-25.
7. Tang W, Shen Z, Guo J, et al. Screening of long non-coding RNA and TUG1 inhibits proliferation with TGF-β induction in patients with COPD. Int J Chron Obstruct Pulmon Dis 2016;11:2951-64.
8. Gu W, Yuan Y, Wang L, et al. Long non-coding RNA TUG1 promotes airway remodelling by suppressing the miR-145-5p/DUSP6 axis in cigarette smoke-induced COPD. J Cell Mol Med 2019;23:7200-9.
9. Huang Y. The novel regulatory role of lncRNA-miRNA-mRNA axis in cardiovascular diseases. J Cell Mol Med 2018;22:5768-75.
10. Liu P, Gao H, Wang Y, et al. LncRNA H19 Contributes to Smoke-Related Chronic Obstructive Pulmonary Disease by Targeting miR-181/PDCD4 Axis. COPD 2023;20:119-25.
11. Zheng ZH, Wu DM, Fan SH, et al. Upregulation of miR-675-5p induced by lncRNA H19 was associated with tumor progression and development by targeting tumor suppressor p53 in non-small cell lung cancer. J Cell Biochem 2019;120:18724-35.
12. Sun YJ, Zhang YF, Xu HM, et al. Morin improves experimental autoimmune thyroiditis in rats via NLRP3/caspase-1 pathway. J Sichuan Univ (Med Sci) 2021;52:229-34.
13. Zhang Z, Liu P, Chen J, et al. Morin ameliorates lung injury in rats with severe pneumonia by inhibiting HMGB1/TLR4/NF-κB pathway. Immunol J 2022;6:478-86.
14. Szoka P, Lachowicz J, Cwiklińska M, et al. Cigarette Smoke-Induced Oxidative Stress and Autophagy in Human Alveolar Epithelial Cell Line (A549 Cells). Adv Exp Med Biol 2019;1176:63-9.
15. Wang L, Yan F, Shi Y, et al. PSAT1 promotes autophagy to resist insufficient autophagy caused by cigarette smoke extract in human airway epithelial cells. Toxicol In Vitro 2024;94:105711.
16. Tulen CBM, Wang Y, Beentjes D, et al. Dysregulated mitochondrial metabolism upon cigarette smoke exposure in various human bronchial epithelial cell models. Dis Model Mech 2022;15:dmm049247.
17. Roscioli E, Jersmann HP, Lester S, et al. Zinc deficiency as a codeterminant for airway epithelial barrier dysfunction in an ex vivo model of COPD. Int J Chron Obstruct Pulmon Dis 2017;12:3503-10.
18. Mizumura K, Cloonan SM, Nakahira K, et al. Mitophagy-dependent necroptosis contributes to the pathogenesis of

COPD. J Clin Invest 2014;124:3987-4003.
19. Wang G, Zhou H, Strulovici-Barel Y, et al. Role of OSGIN1 in mediating smoking-induced autophagy in the human airway epithelium. Autophagy 2017;13:1205-20.
20. Mizumura K, Maruoka S, Shimizu T, et al. Autophagy, selective autophagy, and necroptosis in COPD. Int J Chron Obstruct Pulmon Dis 2018;13:3165-72.
21. Wang H, Mao B, Chen C. Xiaoqinglong Decoction Attenuates Chronic Obstructive Pulmonary Disease in Rats via Inhibition of Autophagy. Evid Based Complement Alternat Med 2018;2018:6705871.
22. McCallum K, Dunning L, McGarvey L, Hollywood M, Brzeszczynska J, Crilly A, Lockhart JC and Litherland GJ. S75 Proteinase activated receptor-2 induced autophagy dysregulation Thorax 2019;74:A49.
23. Zhang K, Zhang PQ, Chen YJ, et al. Effects of lung function of Shenqi Bufei Tang on stable COPD patient with Lung-Qi deficiency syndrome. Chin J Exp Trad Med Formulae 2012;18:213-6.
24. Wu GY, Zhang K, Zhang XY, et al. Effects of Shenqi Bufei Decoction on the expression of HDAC2 and histone acetylation H4 in airway smooth muscle cells proliferation of COPD rat model. Chin J Gerontology 2016; 36:4696-9.
25. Wu G, Zhang K, Yan P, et al. Effects of Shenqi Bufei Decoction on expression of acetylated histone H4, histone deacetylase-2 and nuclear factor-κb p65 in airway smooth muscle of chronic obstructive pulmonary disease rat model with Lung-Qi deficiency syndrome. Tradit Chin Drug Res Clin Pharmacol 2014;25:688-93.
26. Zhang K, Wu G, Zhang X, et al. ShenqiBufei attenuates chronic obstructive pulmonary disease. Int J Clin Exp Med 2017;10:1661-9.
27. Leng A, Yang J, Zhang K. Morin ameliorates chronic obstructive pulmonary disease by inhibiting the expression of MMP9. Acta Universitatis Medicinalis Anhui 2023;58:1987-94.
28. Wang J, Cao B, Han D, et al. Long Non-coding RNA H19 Induces Cerebral Ischemia Reperfusion Injury via Activation of Autophagy. Aging Dis 2017;8:71-84.
29. Ge XJ, Zheng LM, Feng ZX, et al. H19 contributes to poor clinical features in NSCLC patients and leads to enhanced invasion in A549 cells through regulating miRNA-203-mediated epithelial-mesenchymal transition. Oncol Lett 2018;16:4480-8.
30. Wang M, Han D, Yuan Z, et al. Long non-coding RNA H19 confers 5-Fu resistance in colorectal cancer by promoting SIRT1-mediated autophagy. Cell Death Dis 2018;9:1149.
31. Yao D, Jiang Y, Gao S, et al. Deconvoluting the complexity of microRNAs in autophagy to improve potential cancer therapy. Cell Prolif 2016;49:541-53.
32. Lou L, Tian M, Chang J, et al. MiRNA-192-5p attenuates airway remodeling and autophagy in asthma by targeting MMP-16 and ATG7. Biomed Pharmacother 2020;122:109692.
33. Yin H, Zhang S, Sun Y, et al. MicroRNA-34/449 targets IGFBP-3 and attenuates airway remodeling by suppressing Nur77-mediated autophagy. Cell Death Dis 2017;8:e2998.
34. Lin TY, Chan HH, Chen SH, et al. BIRC5/Survivin is a novel ATG12-ATG5 conjugate interactor and an autophagy-induced DNA damage suppressor in human cancer and mouse embryonic fibroblast cells. Autophagy 2020;16:1296-313.
35. Tanida I, Ueno T, Kominami E. LC3 conjugation system in mammalian autophagy. Int J Biochem Cell Biol 2004;36:2503-18.
36. Hsu CC, Hsieh PM, Chen YS, et al. Axl and autophagy LC3 expression in tumors is strongly associated with clinical prognosis of hepatocellular carcinoma patients after curative resection. Cancer Med 2019;8:3453-63.
37. Sun Y, Yao X, Zhang QJ, et al. Beclin-1-Dependent Autophagy Protects the Heart During Sepsis. Circulation 2018;138:2247-62.
38. Kang R, Zeh HJ, Lotze MT, et al. The Beclin 1 network regulates autophagy and apoptosis. Cell Death Differ 2011;18:571-80.
39. Oikonomou P, Giatromanolaki A, Tsaroucha AK, et al. Expression of autophagy-related proteins Beclin-1 and LC3A and proliferation marker Ki-67 in calculous and acalculous human gallbladder epithelium. Hippokratia 2019;23:64-9.
40. Hong S, Li Y, Kaminski PJ, et al. Pathogenesis of Human Papillomaviruses Requires the ATR/p62 Autophagy-Related Pathway. mBio 2020;11:e01628-20.
41. Kumsta C, Chang JT, Lee R, et al. The autophagy receptor p62/SQST-1 promotes proteostasis and longevity in C. elegans by inducing autophagy. Nat Commun 2019;10:5648.
42. Fujii S, Hara H, Araya J, et al. Insufficient autophagy promotes bronchial epithelial cell senescence in chronic obstructive pulmonary disease. Oncoimmunology 2012;1:630-41.
43. Song H, Liu J, Wu X, et al. LHX2 promotes malignancy and inhibits autophagy via mTOR in osteosarcoma and is

negatively regulated by miR-129-5p. Aging (Albany NY) 2019;11:9794-810.
44. Maiese K. New Insights for nicotinamide: Metabolic disease, autophagy, and mTOR. Front Biosci (Landmark Ed) 2020;25:1925-73.
45. Salminen A, Kaarniranta K, Kauppinen A. AMPK and HIF signaling pathways regulate both longevity and cancer growth: the good news and the bad news about survival mechanisms. Biogerontology 2016;17:655-80.
46. Ji L, Li L, Qu F, et al. Hydrogen sulphide exacerbates acute pancreatitis by over-activating autophagy via AMPK/mTOR pathway. J Cell Mol Med 2016;20:2349-61.
47. He Q, Sha S, Sun L, et al. GLP-1 analogue improves hepatic lipid accumulation by inducing autophagy via AMPK/mTOR pathway. Biochem Biophys Res Commun 2016;476:196-203.

Cite this article as: Liu Z, Zeng Y, Li R, Yan Y, Yi S, Zhang K. Treatment of chronic obstructive pulmonary disease by traditional Chinese medicine Morin monomer regulated by autophagy. J Thorac Dis 2024;16(9):6052-6063. doi: 10.21037/jtd-23-1836